

Estimation of Graphical Models using the $L_{1,2}$ Norm

KHAI X. CHIONG[†] AND HYUNGSIK ROGER MOON[‡]

[†]*Naveen Jindal School of Management, University of Texas at Dallas*
E-mail: khai.chiong@utdallas.edu

[‡]*Department of Economics, University of Southern California*
and School of Economics, Yonsei University
E-mail: moonr@usc.edu

Received:

Summary Gaussian graphical models are recently used in economics to obtain networks of dependence among agents. A widely-used estimator is the Graphical Lasso (GLASSO), which amounts to a maximum likelihood estimation regularized using the $L_{1,1}$ matrix norm on the precision matrix Ω . The $L_{1,1}$ norm is a lasso penalty that controls for sparsity, or the number of zeros in Ω . We propose a new estimator called *Structured Graphical Lasso* (SGLASSO) that uses the $L_{1,2}$ mixed norm. The use of the $L_{1,2}$ penalty controls for the *structure* of the sparsity in Ω . We show that when the network size is fixed, SGLASSO is asymptotically equivalent to an infeasible GLASSO problem which prioritizes the sparsity-recovery of high-degree nodes. Monte Carlo simulation shows that SGLASSO outperforms GLASSO in terms of estimating the overall precision matrix and in terms of estimating the structure of the graphical model. In an empirical illustration using a classic firms' investment dataset, we obtain a network of firms' dependence that exhibits the core-periphery structure, with General Motors, General Electric and U.S. Steel forming the core group of firms.

JEL classification: C55, C10.

Keywords: *Gaussian graphical models; Glasso; Inverse covariance matrices; Lasso; Precision matrices; Sparsity.*

1. INTRODUCTION

The Gaussian graphical model is a graph summarizing the conditional independence relationships among a group of random variables. Suppose that (X_1, \dots, X_p) is distributed with $\mathcal{N}(\mathbf{0}, \Sigma_0)$. If the (i, j) -th entry of the precision matrix $\Sigma_0^{-1} \equiv \Omega_0$ is zero, i.e., $\Omega_{0,ij} = 0$, then it is known that X_i and X_j are independent conditional on all other X_k , $k \neq i, j$ (e.g., Chapter 9 of Hastie et al. (2015)). The Gaussian graphical model is then obtained by identifying the zeros of the precision matrix, and letting nodes i and j be linked if and only if the (i, j) -th entry of Ω is non-zero.

In our empirical illustration, the variables (X_1, \dots, X_p) represent the annual investment or the residuals of investment equations of the p number of firms: $(1, \dots, p)$. If two firms i and j are *not* linked in this graphical model, it means that the investment decisions of firms i and j are independent of each other, conditional on all other firms X_k , $k \neq i, j$. Hence the investment decisions of firms i and j do not directly affect each other. On the other hand, if two firms i and j are linked in the graphical model, then the investments of firms i and j have *direct* effects on each other, without the mediation of other firms. In recent applications in economics, for instance, Giudici and Spelta (2016) uses graphical modeling to obtain the network of international financial flows.

It is well known that the inverse of the standard sample covariance estimator, $\hat{\Sigma}^{-1}$, performs poorly particularly in recovering the underlying graphical structure. The reason is that the sample precision matrix produces a dense matrix without any zeros, and hence the resulting graphical model is always a complete network where all nodes are linked to all other nodes.

A widely-used technique to estimate graphical models is called Graphical Lasso (GLASSO), which aims to estimate the precision matrix Ω while imposing a sparsity constraint on Ω . For an overview of this topic, see Hastie et al. (2015); Cai et al. (2016); Fan et al. (2016). In this paper, we propose an estimation method for graphical models, which works by estimating the precision matrix, Ω_0 , taking into account the *structure* of sparsity in Ω_0 .

The standard GLASSO approach estimates the precision matrices while controlling for the sparsity of Ω_0 , i.e. the number of zeros in Ω_0 . However it does not consider when these zeros could be distributed in a certain pattern or structure in Ω_0 . For instance, in many economic applications it is reasonable to think that in the graphical model, some nodes have very few links, while some hub-like nodes have many links to other nodes. Such settings are common in economic applications: for instance, we commonly observe the so-called small-world properties in social and economic networks (Jackson (2008)).

The main feature of our estimation method is to use the $L_{1,2}$ -norm penalty, which corresponds to the second moment of the weighted degree of nodes, i.e. $\sum_{k=1}^p |\Omega_{ik}|$, for $i = 1, \dots, p$. Notice that Lasso uses the $L_{1,1}$ -norm penalty, which is proportional to the first moment of the weighted degree distribution. We derive the asymptotic distribution of the new estimator, called Structured Graphical Lasso (SGLASSO) when the sample size $T \rightarrow \infty$ and the dimension of Ω_0 , p , is fixed.

The main theoretical finding is that when the network size p is fixed, SGLASSO is asymptotically equivalent to an infeasible GLASSO problem which penalizes an entry of Ω proportionally according to the influence of the entry, where the influence of an (i, j) -th entry is defined as the sum of the true weighted degrees of nodes i and j in the graphical model. Specifically, SGLASSO is asymptotically equivalent to a modified GLASSO where the element-by-element penalty factor for the (i, j) -th entry of Ω is proportional to $(d_i + d_j)$, where $d_i = \sum_{k=1}^p |\Omega_{0,ik}|$ is the *true* weighted degree of node i . Note that d_i is unknown to us, and hence it is infeasible to be implemented as a GLASSO estimator.

By means of Monte Carlo simulations, we demonstrate that SGLASSO performs better than GLASSO in finite samples. In terms of estimating the overall precision matrix, SGLASSO achieves lower Kullback-Leibler and Frobenius losses. Moreover, in terms of recovering the structure of the graphical model, we also show that SGLASSO outperforms GLASSO.

Overall, we should use the $L_{1,2}$ norm in cases where we are more interested in the relationships among influential nodes. For instance, in a financial network that exhibits a core-periphery structure, we are more interested in the relationships between the major core banks, and less interested in the relationships between the minor peripheral banks. Knowing how shocks cascade and propagates among influential banks is key to understanding financial contagion (Elliott et al. (2014)).

However if we were to remain completely agnostic about the empirical context, there are still reasons for using the $L_{1,2}$ norm. Here, the virtue of the $L_{1,2}$ norm is that it allows us to express lasso penalties that scale automatically according to degree influences (this insight is due to our main theoretical result). In practice, when we use the $L_{1,2}$ norm in conjunction with the $L_{1,1}$ norm, we are allowing for lasso penalties that have a constant

factor and an increasing factor over the nodes' degrees. This can only improve fit. The analogy is that the $L_{1,1}$ norm is a linear first-order lasso penalty, and the $L_{1,2}$ norm is a quadratic lasso penalty. Moreover, our simulation shows that using just the $L_{1,2}$ norm can achieve significant improvements over the $L_{1,1}$ norm. This suggests that it is important to allow for lasso penalties that scale according to nodes' degrees, and not restricted to a constant lasso penalty.

The paper is organized as follows. Section 2 introduces the model, the $L_{1,2}$ -norm penalty, and a motivating example. Section 3 presents the theoretical results. Section 4 provides a brief summary of the Monte Carlo simulation results. The full simulation results are available in the Supplemental Information. Section 5 contains an empirical illustration. The Appendix contains technical proofs and derivations.

1.1. Related literature

This paper is related to literature of estimating high-dimensional inverse covariance matrices. In addition to the aforementioned surveys, one can refer to Banerjee et al. (2008); Friedman et al. (2008); Yuan and Lin (2007); Rothman et al. (2008); Ravikumar et al. (2011).

A different class of procedure frames the estimation of graphical models as nodewise or pairwise regressions, where the Lasso or Dantzig selector can then be used to achieve variable selection and high-dimensional regularization. The relevant papers belonging to this class are Cai et al. (2011, 2016); Meinshausen and Bühlmann (2006); Peng et al. (2012); Ren et al. (2015). For ultra high-dimensional Gaussian graphical models, a recent approach is the Innovated Scalable Efficient Estimation proposed by Fan and Lv (2016).

Lam and Fan (2009) study a general class of estimators that nests the GLASSO. In particular, they consider $\operatorname{argmax}_{\Omega \succ 0} \{ \log \det \Omega - \operatorname{tr}(\Omega \hat{\Sigma}) - \sum_{i \neq j} p_\lambda(|\Omega_{ij}|) \}$, where $p_\lambda(\cdot)$ is a penalty function that depends on a regularization parameter λ . The SGLASSO estimator does not belong to this class because our penalty term $\|\Omega\|_{1,2}^2$ is not additively separable in the entries of Ω . Hence, SGLASSO cannot be analyzed using the framework proposed in Lam and Fan (2009).¹

Another type of mixed norm that is widely used in the high-dimensional linear regression setting is the $L_{2,1}$ -norm, also known as the Group Lasso (Friedman et al. (2010); Yuan and Lin (2006)), which is useful when parameters are naturally partitioned into disjoint groups, and we would like to achieve sparsity with respect to whole groups. In contrast, our proposed $L_{1,2}$ -norm is distinct from the $L_{2,1}$ -norm, and has not been studied in the context of covariance estimation.

2. SETUP

Let $\mathbf{X} = (X_1, \dots, X_p) \in \mathbb{R}^p$ be a p -dimensional vector distributed according to a multivariate distribution with mean zero and covariance matrix Σ_0 . Our goal is to obtain the graphical model corresponding to \mathbf{X} , which is defined as follows.

The (Gaussian) graphical model of \mathbf{X} is an undirected graph $G = (V, E)$. The set of nodes (or vertices) of this graph is $V = \{1, \dots, p\}$. Each node i corresponds to a

¹It is possible to incorporate other penalty functions into our estimator. Consider: $\hat{\Omega}_{\text{sc-glasso}} := \operatorname{argmax}_{\Omega \succ 0} \{ \log \det \Omega - \operatorname{tr}(\Omega \hat{\Sigma}) - \|p_\lambda(\Omega)\|_{1,2}^2 \}$, where $p_\lambda(\Omega)$ denotes the matrix (of the same dimension as Ω) such that $p_\lambda(\Omega)_{ij} = p_\lambda(\Omega_{ij})$. For instance, we can then let $p_\lambda(\cdot)$ to be the Smoothly Clipped Absolute Deviation (SCAD) penalty function (Fan and Li (2001)).

random variable X_i . The set of links (or edges) E is such that $\{i, j\} \notin E$ if and only if $X_i \perp X_j$ conditional on all $X_k, k \in V \setminus \{i, j\}$. That is, the graphical model is defined such that there is *no* link between nodes i and j in the graph if and only if X_i and X_j are independent conditional on all other nodes besides i and j . As such the graphical model G summarizes the pairwise conditional independence relationships among (X_1, \dots, X_p) . The existence of a link in G amounts to conditional dependence between the two nodes given all other ones.

Estimation of graphical models is based on the following known fact: if \mathbf{X} is Gaussian, then the non-zeros in its precision matrix (or inverse covariance matrix) $\Omega_0 := \Sigma_0^{-1}$ corresponds exactly to links in the graphical model (see Hastie et al. (2015); Whittaker (2009)). That is, there is a link between nodes i and j if and only if the (i, j) -th entry of Ω_0 is non-zero. Similarly the lack of a link $\{i, j\}$ between a pair of nodes i and j is equivalent to the (i, j) -th entry of Ω_0 being zero.

Now suppose we observe T i.i.d samples $\mathbf{X}_t, t = 1, \dots, T$ from $\mathbf{X} = (X_1, \dots, X_p)$. We now introduce the GLASSO estimator, as well as our proposed SGLASSO estimator, that allows us to recover the graphical model from the samples. The output of these estimators is a sparse precision matrix $\hat{\Omega}$. From $\hat{\Omega}$, the estimated graphical model is then constructed by including a link between nodes i and j if and only if $\hat{\Omega}_{i,j} \neq 0$.

For a $m \times n$ matrix A , define the mixed $L_{p,q}$ norm as follows:

$$\|A\|_{p,q} = \left[\sum_{j=1}^n \left(\sum_{i=1}^m |a_{ij}|^p \right)^{q/p} \right]^{1/q}.$$

The following $L_{1,2}$ norm in equation (2.1) will play a crucial role in our estimator:

$$\|A\|_{1,2} = \left[\sum_{j=1}^n \left(\sum_{i=1}^m |a_{ij}| \right)^2 \right]^{1/2}. \quad (2.1)$$

Our **Structured-GLASSO** (SGLASSO) estimator is defined in equation (2.2) below, where $\hat{\Sigma}$ is the sample covariance matrix calculated from the sample $(\mathbf{X}_t)_{t=1}^T$.

$$\hat{\Omega}_{\text{sglasso}} := \underset{\Omega > 0}{\operatorname{argmax}} \left\{ \log \det \Omega - \operatorname{tr}(\Omega \hat{\Sigma}) - \lambda_T \|\Omega\|_{1,2}^2 \right\}. \quad (2.2)$$

In comparison, the **GLASSO** estimator (Banerjee et al. (2008); Friedman et al. (2008); Yuan and Lin (2007); Fan et al. (2015)) is defined in equation (2.3). While SGLASSO uses the $L_{1,2}$ mixed norm as a penalty to the likelihood, GLASSO in equation (2.3) uses the $L_{1,1}$ norm, which is the familiar lasso penalty (sum of the absolute values of the entries of Ω).

$$\hat{\Omega}_{\text{glasso}} := \underset{\Omega > 0}{\operatorname{argmax}} \left\{ \log \det \Omega - \operatorname{tr}(\Omega \hat{\Sigma}) - \lambda_T \|\Omega\|_{1,1} \right\}. \quad (2.3)$$

Another definition of the GLASSO is one where only Ω^- is penalized, where Ω^- denotes the matrix Ω where its' diagonal entries are set to zero. While Yuan and Lin

(2007); Rothman et al. (2008) use equation (2.3), other authors such as Banerjee et al. (2008); Friedman et al. (2008) use the latter. For various expositional reasons, we will penalize Ω instead of Ω^- . However in the Monte Carlo simulation, we will also compare with the variant of GLASSO where the diagonals are not penalized.

Although we are comparing SGLASSO with GLASSO in this paper, we could also combine them together. That is, $\hat{\Omega} := \operatorname{argmax}_{\Omega \succ 0} \{ \log \det \Omega - \operatorname{tr}(\Omega \hat{\Sigma}) - \lambda_{1T} \|\Omega\|_{1,1} - \lambda_{2T} \|\Omega\|_{1,2}^2 \}$, and use cross-validation procedures to tune the parameters λ_{1T} and λ_{2T} .

We do not require that the data-generating process be Gaussian.² Therefore our estimator can be seen as maximizing a Gaussian quasi-likelihood subject to regularization. When there is no penalty ($\lambda_T = 0$), then $\hat{\Omega}$ defined in both (2.2) and (2.3) correspond to the Quasi Maximum Likelihood estimator of the inverse covariance matrix, which is given by the inverse of the empirical sample covariance matrix. As we mentioned in the introduction, it is well-known that the unpenalized sample estimator behaves poorly, and it is unsuitable for graphical modeling when zeros of the estimates are important.

2.1. Motivating Example

We illustrate the difference between the $L_{1,2}$ and the conventional $L_{1,1}$ lasso norms. Define Ω_1 and Ω_2 as the precision matrices given by equations (2.4) and (2.5) below.

$$\Omega_1 = \begin{bmatrix} 1 & \frac{1}{\sqrt{5}} & \frac{1}{\sqrt{5}} & \frac{1}{\sqrt{5}} & \frac{1}{\sqrt{5}} \\ \frac{1}{\sqrt{5}} & 1 & 0 & 0 & 0 \\ \frac{1}{\sqrt{5}} & 0 & 1 & 0 & 0 \\ \frac{1}{\sqrt{5}} & 0 & 0 & 1 & 0 \\ \frac{1}{\sqrt{5}} & 0 & 0 & 0 & 1 \end{bmatrix} \quad (2.4) \quad \Omega_2 = \begin{bmatrix} 1 & \frac{1}{\sqrt{5}} & 0 & 0 & 0 \\ \frac{1}{\sqrt{5}} & 1 & \frac{1}{\sqrt{5}} & 0 & 0 \\ 0 & \frac{1}{\sqrt{5}} & 1 & \frac{1}{\sqrt{5}} & 0 \\ 0 & 0 & \frac{1}{\sqrt{5}} & 1 & \frac{1}{\sqrt{5}} \\ 0 & 0 & 0 & \frac{1}{\sqrt{5}} & 1 \end{bmatrix} \quad (2.5)$$

The precision matrices Ω_1 and Ω_2 give rise respectively to the graphical models in Figure 1 and Figure 2 below, where links in the graphs represent non-zero entries in the precision matrices.

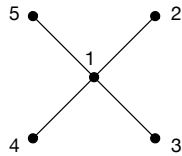


Figure 1: Ω_1 : star graph

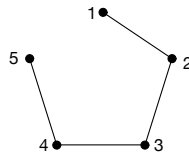


Figure 2: Ω_2 : AR(1) model.

Both the standard Lasso and Frobenius norms do not distinguish between Ω_1 and Ω_2 , while our proposed $L_{1,2}$ -norm does. The reason is clear: both Ω_1 and Ω_2 have the same number of zeros. They have the same sparsity but the structure of this sparsity is very

²When the DGP is non-Gaussian, the graphical model estimated using GLASSO or SGLASSO is still useful – it corresponds to the structure of pairwise conditional correlations (partialling out other variables).

different. For the $L_{1,1}$ lasso norm, we have: $L_{1,1}(\Omega_1) = L_{1,1}(\Omega_2) = \sum_{j=1}^p \sum_{i \neq j}^p |\frac{1}{\sqrt{5}}| + 5 = \frac{8}{\sqrt{5}} + 5$. Similarly, for the $L_{2,2}$ Frobenius norm, we have $L_{2,2}(\Omega_1) = L_{2,2}(\Omega_2)$.

Now on the other hand, the $L_{1,2}$ -norm can distinguish between these two structures. The $L_{1,2}$ norm evaluated at Ω_1 for the star graph is $\|\Omega_1\|_{1,2}^2 \approx 16.16$. While the $L_{1,2}$ norm evaluated at Ω_2 for the AR(1) graph is $\|\Omega_2\|_{1,2}^2 \approx 14.96$.

3. THEORETICAL PROPERTIES

In this section we derive the limiting distribution of SGLASSO when the number of samples T goes to infinity while p is fixed (following Yuan and Lin (2007)). The main finding of this section is that SGLASSO is asymptotically equivalent to an infeasible GLASSO problem which prioritizes the sparsity-recovery of high-degree nodes. More precisely, we show that SGLASSO is asymptotically equivalent to a modified GLASSO estimator where each row of Ω is penalized proportionally according to its *true* degree. The true degree of row (or node) i is defined by $d_i = \sum_{j=1}^p |\Omega_{0,ij}|$. The term “degree” should be understood as “weighted degree” henceforth.

This asymptotic equivalence result has two implications. First, SGLASSO inherits the sparsity-discovery property of GLASSO where zeros in the precision matrix are estimated precisely to be zero (due to the non-differentiability of the penalty function at zeros). Therefore SGLASSO estimates are also sparse. Secondly, SGLASSO differs from GLASSO in that it prioritizes recovering the zero-pattern of high-degree nodes. Nodes with higher weighted degrees can be viewed as being more influential and important, and we might be more interested in uncovering the relationships among influential agents.

To derive the limiting distributions of our SGLASSO estimator, we assume a high level assumption on the weak limit of the sample covariance matrix.

ASSUMPTION 3.1. *We assume that*

$$\text{vech}(\sqrt{T}(\hat{\Sigma} - \Sigma_0)) \Rightarrow \text{vech}(W) \sim \mathcal{N}(0, \Lambda),$$

where the notation *vech* is the half-vectorization operator that takes only the lower-triangular part of a symmetric matrix.

This high level condition holds when $X_{j,t}X_{k,t}$ have higher moments and the serial dependence is weak. When $\mathbf{X}_t \sim_{i.i.d.} \mathcal{N}(0, \Sigma_0)$, then $\sqrt{T}(\text{vech}(\hat{\Sigma} - \Sigma_0)) \Rightarrow \text{vech}(W) \sim \mathcal{N}(0, \Lambda)$, where Λ is such that $\text{Cov}(W_{ij}, W_{i'j'}) = \text{Cov}(X_{i,t}X_{j,t}, X_{i',t}X_{j',t})$.

Now let D_p be a $p \times p$ matrix whose (i, j) entry is $d_j \equiv \sum_{k=1}^p |\Omega_{0,jk}|$, the true weighted degree of node j . Define

$$\hat{\Omega}_{D_p} = \underset{\Omega \succ 0}{\text{argmax}} \{ \log \det \Omega - \text{tr}(\Omega \hat{\Sigma}) - 2\lambda_T \|D_p \circ \Omega\|_{1,1} \} \quad (3.6)$$

to be a variant of the GLASSO estimator. Here, the operator \circ is the element-wise multiplication. The SGLASSO estimator is defined as: $\hat{\Omega}_\lambda = \underset{\Omega \succ 0}{\text{argmax}} \{ \log \det \Omega - \text{tr}(\Omega \hat{\Sigma}) - \lambda_T \|\Omega\|_{1,2}^2 \}$.

THEOREM 3.1. *Suppose that as $T \rightarrow \infty$, $\sqrt{T}\lambda_T \rightarrow \lambda_0 > 0$. Then,*

$$\sqrt{T}(\hat{\Omega}_\lambda - \Omega_0) = \sqrt{T}(\hat{\Omega}_{D_p} - \Omega_0) + o_p(1).$$

In addition, suppose that Assumption 3.1 holds. Then,

$$\sqrt{T}(\hat{\Omega}_\lambda - \Omega_0), \text{ and } \sqrt{T}(\hat{\Omega}_{D_p} - \Omega_0) \Rightarrow \underset{U \in \mathbb{R}^{p \times p}}{\operatorname{argmin}} V(U),$$

where

$$V(U) = \operatorname{tr}(U\Sigma_0U\Sigma_0) + \operatorname{tr}(UW) + 2\lambda_0 \sum_{i=1}^p \sum_{j=1}^p g_{ij}(u_{ij})d_j \quad (3.7)$$

as $T \rightarrow \infty$. Here $\Sigma_0 = \Omega_0^{-1}$ is the true covariance matrix of X , and $g_{ij}(u) := u \operatorname{sign}(\Omega_{0,ij})\mathbb{1}(\Omega_{0,ij} \neq 0) + |u|\mathbb{1}(\Omega_{0,ij} = 0)$.

Compared to the limit in Theorem 3.1, the GLASSO estimator has the following limiting distribution (Yuan and Lin (2007))³:

$$\underset{U \in \mathbb{R}^{p \times p}}{\operatorname{argmin}} V_{\text{glasso}}(U)$$

where

$$V_{\text{glasso}}(U) = \operatorname{tr}(U\Sigma_0U\Sigma_0) + \operatorname{tr}(UW) + \lambda_0 \sum_{i=1}^p \sum_{j=1}^p g_{ij}(u_{ij}) \quad (3.8)$$

where $\sqrt{T}\lambda_T \rightarrow \lambda_0$.

Comparing equations (3.7) and (3.8), we see that the SGLASSO obtains the same limiting distribution as that of a modified GLASSO with element-wise LASSO penalty given by $2\|D_p \circ \Omega\|_{1,1}$. Since D_p is constructed using the true, unknown values of Ω_0 , SGLASSO cannot be simply implemented as GLASSO.

Moreover from Proposition 3.1 below, we can further say that SGLASSO is asymptotically equivalent to a variant of GLASSO where the penalty term is $\sum_{i=1}^p \sum_{j=1}^p (d_i + d_j)|\Omega_{ij}|$. That is, each entry Ω_{ij} is given the penalty factor equals to the sum of the (true) weighted degrees of nodes i and j .

PROPOSITION 3.1. *Let D_p be a $p \times p$ matrix whose (i, j) entry is $d_j \equiv \sum_{k=1}^p |\Omega_{0,jk}|$. It is true that $2\|D_p \circ \Omega\|_{1,1} = \sum_{i=1}^p \sum_{j=1}^p (d_i + d_j)|\Omega_{ij}|$.*

All proofs are relegated to the Appendix. In the Supporting Information, we plot and illustrate the asymptotic distribution in Theorem 3.1. We show that with a higher probability, SGLASSO correctly estimates a non-link (a zero entry) belonging to a high-degree node.

The distribution of $\underset{U \in \mathbb{R}^{p \times p}}{\operatorname{argmin}} V(U)$ can be simulated after replacing the unknown components Σ_0 , Ω_0 , and Λ with their consistent estimates, and this can be used in inference procedures on Ω_0 .

A noticeable feature, however, is that the limit distribution in Theorem 3.1 is discontinuous with respect to true DGP. This is because $g_{ij}(u)$ is discontinuous as a function of $\Omega_{0,ij}$ at $\Omega_{0,ij} = 0$. This implies that the inference based on this limit would only be valid pointwise, not uniformly in Ω_0 .⁴

³Yuan and Lin (2007) consider the GLASSO estimator where the diagonals are not penalized, so that $V_{\text{glasso}}(U) = \operatorname{tr}(U\Sigma_0U\Sigma_0) + \operatorname{tr}(UW) + \lambda_0 \sum_{i=1}^p \sum_{j \neq i}^p g(u_{ij})$ in their paper.

⁴See Belloni et al. (2014) and Van de Geer et al. (2014). We thank one of the referees who pointed this out.

4. SIMULATION RESULTS

We compare our estimator against GLASSO by considering 3 different graphical models here. In the Supplemental Information, we consider 8 other models. The first two models are depicted in Figure 3. The last model is the graphical model calibrated to the empirical application as depicted in Figure 5. From a given graphical model, we generate the true precision matrix Ω_0 such that $\Omega_{0,ij} = 0$ if and only if there is a link between nodes i and j , otherwise we set $\Omega_{0,ij} = 0.2$. We set $\Omega_{0,ii} = 1$.

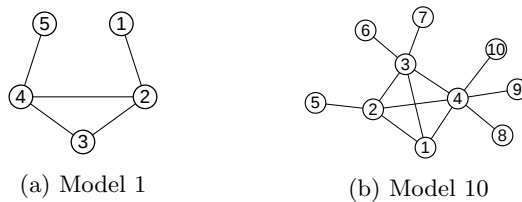


Figure 3: $p = 5$ and $= 10$

For each model, we draw 1,000 independent datasets from $\mathcal{N}(0, \Omega_0^{-1})$. That is, each dataset comprises of $(\mathbf{X}_t)_{t=1}^T$, where $\mathbf{X}_t \in \mathbb{R}^p$ is randomly drawn from $\mathcal{N}(0, \Omega_0^{-1})$. For the sample size, we consider $T = 20$ and $T = 50$.

Both estimators involve choosing the λ_T tuning parameters. We use a 2-folds cross-validation procedure to tune λ_T . Specifically, we use the Kullback-Leibler (KL) loss averaged over the two-folds to evaluate predictive accuracies. Equation (3.18) gives the KL loss between the estimated $\hat{\Omega}$ from the training set versus the estimated Ω from the validation set:

$$KL(\lambda_T) = \log \det(\Omega) - \log \det \hat{\Omega} + \text{tr}(\hat{\Omega}\Omega^{-1}) - p \quad (4.9)$$

We report the simulation result in Table 1. In the table, the (a) columns corresponds to SGLASSO whereas the (b) columns refer to GLASSO. In Columns 1(a) and 1(b), we report the optimal λ_T as determined by cross-validations, averaged across the 1,000 replications. In Columns 2(a) and 2(b), we report the Kullback-Leibler loss averaged across 1,000 replications.⁵ In Columns 3(a) and 3(b), we report the average Frobenius loss between $\hat{\Omega}$ and Ω_0 .

In the last two columns of Table 1, we report the F_1 score, which measures the accuracy of graph recovery. The Kullback-Leibler loss and the Frobenius norms may not fully capture how accurately the zeros are recovered. We introduce an additional metric: $F_1 = \frac{2 \text{precision} \cdot \text{recall}}{\text{precision} + \text{recall}}$, where *precision* is the ratio of true positives (TP) to all predicted positives (TP + FP), *recall* is the ratio of true positives to all actual positives (TP + FN). Alternatively, the F_1 score can be written as $F_1 = \frac{2TP}{2TP + FP + FN}$. The F_1 score measures the quality of a binary classifier by equally balancing both the precision and the recall of a classifier. The larger the F_1 score is, the better the classifier is. The F_1 score is commonly used in machine learning to evaluate binary classifiers. For instance, the Yelp competition uses the F_1 score as a metric to rank competing models.⁶ The F_1 score is favored over the metric $Accuracy = \frac{TP + TN}{TP + TN + FP + FN}$ especially in our current setting

⁵The KL loss between $\hat{\Omega}$ and Ω_0 is given by $KL(\hat{\Omega}, \Omega_0) = \log \det(\Omega_0) - \log \det \hat{\Omega} + \text{tr}(\hat{\Omega}\Omega_0^{-1}) - p$

⁶<https://www.kaggle.com/c/yelp-restaurant-photo-classification>

where the graphical models are sparse. This is because a model that naively predicts all negatives will obtain a high *Accuracy* score just because there are many actual negatives, and the TN term dominates the *Accuracy* score.

| Model | T | Optimal λ_T | | KL | | Frobenius | | F_1 score | |
|-------|-----|---------------------|------------------|------------------|------------------|------------------|------------------|------------------|------------------|
| | | (a) SGLASSO | (b) GLASSO | (a) SGLASSO | (b) GLASSO | (a) SGLASSO | (b) GLASSO | (a) SGLASSO | (b) GLASSO |
| (1) | 20 | 0.181 (0.118) | 0.342 (0.133) | 0.430 (0.207) | 0.483 (0.215) | 0.896 (0.223) | 0.948 (0.214) | 0.439 (0.248) | 0.367 (0.259) |
| (10) | 20 | 0.207 (0.094) | 0.399 (0.109) | 0.946 (0.278) | 1.096 (0.527) | 1.353 (0.183) | 1.456 (0.414) | 0.336 (0.143) | 0.272 (0.162) |
| (11) | 20 | 0.198 (0.097) | 0.389 (0.117) | 1.201 (0.312) | 1.390 (0.723) | 1.569 (0.186) | 1.701 (0.522) | 0.403 (0.143) | 0.341 (0.164) |
| (1) | 50 | 0.088 (0.054) | 0.179 (0.076) | 0.246 (0.084) | 0.265 (0.091) | 0.710 (0.129) | 0.736 (0.134) | 0.564 (0.225) | 0.541 (0.248) |
| (10) | 50 | 0.109 (0.040) | 0.230 (0.052) | 0.593 (0.115) | 0.651 (0.128) | 1.137 (0.113) | 1.190 (0.117) | 0.466 (0.136) | 0.437 (0.159) |
| (11) | 50 | 0.091 (0.041) | 0.206 (0.053) | 0.747 (0.153) | 0.807 (0.167) | 1.312 (0.128) | 1.370 (0.133) | 0.563 (0.120) | 0.541 (0.137) |

Table 1: Averages and standard errors from 1,000 replications.

The conclusion from Table 1 is that SGLASSO achieves significantly lower Kullback-Leibler and Frobenius losses. Moreover in terms of graph accuracy, SGLASSO also outperforms GLASSO, as indicated by the F_1 scores.

To abstract away from the effects of cross-validations, we consider the lowest Kullback-Leibler losses that can be achieved by our estimator versus the GLASSO. Specifically, we vary λ_T and at each λ_T , we compute the KL and Frobenius losses between the true Ω_0 and $\hat{\Omega}$. We see from Table 7 that the superior performance of SGLASSO over GLASSO exists after taking away the randomness due to cross-validations. The lowest possible KL losses achievable by our estimator appears to be smaller, than the corresponding KL losses for the GLASSO.

Theorem 3.1 says that the SGLASSO prioritizes recovering the sparsity between nodes that have higher degrees. We now show some numerical evidence that lends support to this. For each model, we examined the pair of nodes (i, j) such that $d_i + d_j$ is largest and $\Omega_{0,ij} = 0$, where $d_i = \sum_{k=1}^p |\Omega_{0,ik}|$ is the true weighted degree of node i . For instance, for model 1, the $\operatorname{argmax}_{i,j} (d_i + d_j)$ such that $\Omega_{0,ij} = 0$ would correspond to the pairs of nodes $(1, 4)$ and $(2, 5)$. For simplicity, if there are multiple pairs of nodes that maximize $d_i + d_j$, we will pick the pair of nodes that comes first when the adjacency matrix is vectorized.

In each of the model (set $T = 20$), we calculate the fraction of times that GLASSO and SGLASSO correctly recover $\Omega_{0,ij} = 0$ for the largest $d_i + d_j$. We plot this result in Figure 11, which shows that at any given λ , the probability of correctly recovering $\Omega_{0,ij} = 0$ for high-degree nodes is greater when SGLASSO is used, compared to GLASSO.

4.1. Computational details

Computing the SGLASSO estimator is a convex optimization problem. More precisely, the problem consists of minimizing a smooth convex term given by $-\log \det \Omega + \operatorname{tr}(\Omega \hat{\Sigma})$,

| Model | T | Minimum KL | | Minimum Frobenius | | Percentage Dominance |
|-------|-----|------------------|------------------|-------------------|------------------|----------------------|
| | | (a) | (b) | (a) | (b) | |
| | | SGLASSO | GLASSO | SGLASSO | GLASSO | |
| (1) | 20 | 0.340 (0.106) | 0.376 (0.120) | 0.779 (0.096) | 0.821 (0.116) | 0.99 |
| (10) | 20 | 0.824 (0.162) | 0.887 (0.176) | 1.234 (0.085) | 1.279 (0.101) | 0.99 |
| (11) | 20 | 1.041 (0.191) | 1.102 (0.205) | 1.415 (0.087) | 1.466 (0.101) | 0.95 |
| (1) | 50 | 0.199 (0.063) | 0.211 (0.065) | 0.606 (0.095) | 0.634 (0.098) | 0.92 |
| (10) | 50 | 0.509 (0.087) | 0.533 (0.095) | 1.021 (0.072) | 1.035 (0.082) | 0.96 |
| (11) | 50 | 0.652 (0.104) | 0.675 (0.114) | 1.203 (0.067) | 1.204 (0.082) | 0.86 |

Table 2: Minimum possible KL and Frobenius losses across all λ_T (averages and standard errors from 1,000 replications). In the last column, we report the fraction of times in which SGLASSO performed better in terms of KL loss at the corresponding λ_T .

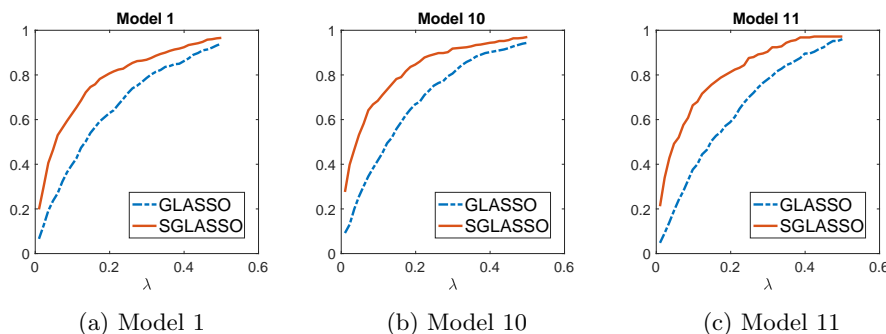


Figure 4: Each figure shows the estimated probability of recovering the non-link (i, j) such that $(d_i + d_j)$ is the largest in each model, as a function of the tuning parameter λ_T .

and a non-differentiable convex term corresponding to $\lambda_T \|\Omega\|_{1,2}^2$. Since the objective can be formulated as minimizing the sum of a differentiable convex function and a non-differentiable convex function, we can use the *proximal gradient method* (Beck and Teboulle (2009)) to compute SGLASSO.

In this paper, we use CVX, a Matlab package for specifying and solving convex programs (Grant et al. (2008)). CVX supports convex objective functions that are non-smooth (Grant and Boyd (2008)). CVX also allows us to easily enforce symmetry and positive-definiteness of the matrix minimand, which is needed here. The code is readily available from the authors upon request.

5. EMPIRICAL ILLUSTRATION

For a real-world empirical illustration, we use the classic Grunfeld investment data (see Greene (2012) or Baltagi (2008)). The goal is to estimate the network dependence structure of firms' investment decision.⁷

The data consist of time series of $T = 20$ yearly observations on $p = 10$ firms. The three variables are I_{it} = real gross investment of firm i in year t , F_{it} = real market value of the firm, C_{it} = real value of capital stock such as plant and equipment.

The investment decision for firm i is modeled as follows: $I_{it} = \beta_{1i} + \beta_{2i}F_{it} + \beta_{3i}C_{it} + \epsilon_{it}$, where $(\epsilon_{1t}, \epsilon_{2t}, \dots, \epsilon_{pt}) \sim iid(0, \Omega_0^{-1})$. The zeros and non-zeros in Ω_0 correspond to the dependence structure of firms' investment decisions (the object of interest here).

For each firm i , we first estimate the linear equation: $I_{it} = \beta_{1i} + \beta_{2i}F_{it} + \beta_{3i}C_{it} + \epsilon_{it}$. This is also the first step in the estimation of Seemingly Unrelated Regressions. Secondly, we use our proposed SGLASSO to estimate the precision matrix of the first-step residuals $\hat{\epsilon}_{it}$, $i = 1, \dots, 10$, $t = 1, \dots, 20$. The tuning parameter is determined using a two-fold cross-validation procedure. The result is shown in Figure 5. (We also estimated the graphical model corresponding to the observed investment variable I_{it} , the result is similar)

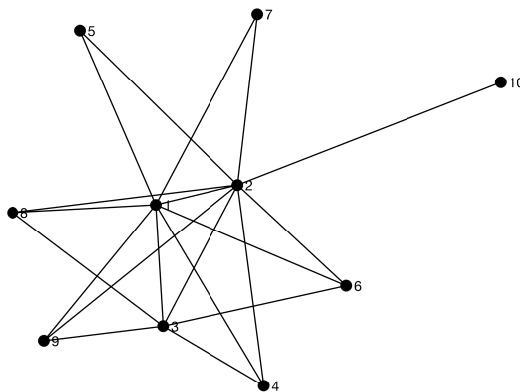


Figure 5: Network of firms' dependence estimated using SGLASSO. The estimated graphical model exhibits a clear core-periphery structure. The core firms are 1, 2 and 3, which are respectively General Motors, U.S. Steel and General Electric. The periphery firms do not have links to each other, but are linked only to the core firms. All core firms are linked to each other.

The recovered graphical model exhibits a clear core-periphery structure. There are two groups of firms: a group of core firms and a group of periphery firms. The core firms are linked to each other, as well as linked to the periphery firms. The periphery firms however, are *not* linked to each other, but are only linked to the core firms. Therefore every node is linked directly to a core firm. The core firms here are firms 1, 2 and 3, which are respectively General Motors, U.S. Steel and General Electric. Using the GLASSO estimator, we recover an identical graphical model – the finding is robust to different choices of penalty functions.

⁷The data can be downloaded freely from Greene (2012)'s companion website.

Finally we cannot recover this core-periphery structure using the sample estimator (without regularization). To show this, we estimate the sample precision matrix of the residual estimates $\hat{\epsilon}_{it}$ from the first step. The graphical model corresponding to this sample precision matrix is the complete graph, where every node is linked to all other nodes – the sample precision matrix is dense and do not contain any zeros.

6. CONCLUDING REMARKS AND POLICY IMPLICATIONS

Graphical model is a potentially useful tool for economists. Using graphical models, we can obtain the network of dependence among random variables. We introduce Structured Graphical Lasso (SGLASSO) as an estimator of graphical models. Using a classic firms' investment dataset, we find that the dependence structure of firms' investment decision exhibits a core-periphery network. This has some relevant policy implications – small shocks to those core firms will affect the entire network, creating large aggregate fluctuations as in Acemoglu et al. (2012). Indeed per our finding, one of the core firms is General Motors, whose Chapter 11 restructuring posed a systemic risk to the U.S. economy in 2009.

ACKNOWLEDGEMENTS

We thank Victor Chernozhukov and two referees for helpful comments and suggestions. The first draft of the paper was written while Moon and Chiong were Associate Director and a postdoctoral fellow of USC Dornsife INET, respectively. Moon acknowledges that this work was supported by the Ministry of Education of the Republic of Korea and the National Research Foundation of Korea (NRF-2017S1A5A2A01023679).

APPENDIX

A. PROOFS

We will use the following important result that concerns the asymptotics of the minimizer of a convex random function (Geyer (1994); Hjort and Pollard (2011); Kato (2009); Pollard (1991)).

LEMMA 1.1. *Let $f_n(\mathbf{x}, \Omega) : \mathbb{R}^d \times \Omega \rightarrow \mathbb{R}$ be a random convex function, that is, $f_n(\mathbf{x}, \cdot)$ is a random variable for each $\mathbf{x} \in \mathbb{R}^d$. Moreover, let $\mathbf{x}_n^*(\Omega)$ be the unique minimizer of $f_n(\mathbf{x}, \Omega)$ with respect to \mathbf{x} . Suppose that $f_n(\mathbf{x}, \cdot)$ converges in distribution to some random convex function $f_\infty(\mathbf{x}, \cdot)$ for each \mathbf{x} . Now if $\mathbf{x}_\infty^*(\Omega)$ is the unique minimizer of $f_\infty(\mathbf{x}, \Omega)$, then the random variable \mathbf{x}_n^* converges in distribution to the random variable \mathbf{x}_∞^* .*

A.1. Proof of Theorem 3.1

To prove Theorem 3.1, define the following convex random functions by re-parameterization $U = \sqrt{T}(\Omega - \Omega_0)$:

$$\begin{aligned} V_T(U) = & -\log \det \left(\Omega_0 + \frac{U}{\sqrt{T}} \right) + \text{tr} \left\{ \left(\Omega_0 + \frac{U}{\sqrt{T}} \right) \hat{\Sigma} \right\} + \lambda_T \left\| \Omega_0 + \frac{U}{\sqrt{T}} \right\|_{1,2}^2 \\ & + \log \det \Omega_0 - \text{tr}(\Omega_0 \hat{\Sigma}) - \lambda_T \|\Omega_0\|_{1,2}^2, \end{aligned} \tag{1.10}$$

and

$$\begin{aligned} V_T^l(U) &= -\log \det \left(\Omega_0 + \frac{U}{\sqrt{T}} \right) + \text{tr} \left\{ \left(\Omega_0 + \frac{U}{\sqrt{T}} \right) \hat{\Sigma} \right\} + 2\lambda_T \left\| D_p \circ \left(\Omega_0 + \frac{U}{\sqrt{T}} \right) \right\|_{1,1} \\ &\quad + \log \det \Omega_0 - \text{tr}(\Omega_0 \hat{\Sigma}) - 2\lambda_T \|D_p \circ \Omega_0\|_{1,1}. \end{aligned} \quad (1.11)$$

This function is random because of its dependence on the sample covariance matrix, $\hat{\Sigma}$. By definition, our SGLASSO estimator $\hat{\Omega}_\lambda$ satisfies the following.

$$\sqrt{T}(\hat{\Omega}_\lambda - \Omega_0) = \hat{U} := \underset{U}{\text{argmin}} V_T(U).$$

By Lemma 1.1, the limit distribution of $\sqrt{T}(\hat{\Omega}_\lambda - \Omega_0)$ follows if we show

$$TV_T(U) \rightarrow V(U), \quad (1.12)$$

as $T \rightarrow \infty$ and as $\sqrt{T}\lambda_T \rightarrow \lambda_0 \geq 0$, where the random limit function $V(U)$ is defined in equation (3.7).

Following the argument in the proof of Theorem 1 of Yuan and Lin (2007), we have that:

$$\log \det \left(\Omega_0 + \frac{U}{\sqrt{T}} \right) - \log \det \Omega_0 = \frac{\text{tr}(U\Sigma_0)}{\sqrt{T}} - \frac{\text{tr}(U\Sigma_0 U\Sigma_0)}{T} + o\left(\frac{1}{T}\right) \quad (1.13)$$

$$\begin{aligned} \text{tr} \left\{ \left(\Omega_0 + \frac{U}{\sqrt{T}} \right) \hat{\Sigma} \right\} - \text{tr}(\Omega_0 \hat{\Sigma}) &= \text{tr} \left(\frac{U\hat{\Sigma}}{\sqrt{T}} \right) \\ &= \text{tr} \left(\frac{U\Sigma_0}{\sqrt{T}} \right) + \text{tr} \left(\frac{U(\hat{\Sigma} - \Sigma_0)}{\sqrt{T}} \right) \end{aligned} \quad (1.14)$$

Moreover, we know that when T is large enough,

$$\left| \Omega_{0,ij} + \frac{u_{ij}}{\sqrt{T}} \right| - |\Omega_{0,ij}| = \frac{g_{ij}}{\sqrt{T}}$$

where $g_{ij} = u_{ij} \text{sign}(\Omega_{0,ij}) \mathbb{1}(\Omega_{0,ij} \neq 0) + |u_{ij}| \mathbb{1}(\Omega_{0,ij} = 0)$. Therefore we can show that the difference of the penalty terms can be written as

$$\begin{aligned} \left\| \Omega_0 + \frac{U}{\sqrt{T}} \right\|_{1,2}^2 - \|\Omega_0\|_{1,2}^2 &= \sum_{j=1}^p \left(\sum_{i=1}^p \left| \Omega_{0,ij} + \frac{u_{ij}}{\sqrt{T}} \right| \right)^2 - \sum_{j=1}^p \left(\sum_{i=1}^p |\Omega_{0,ij}| \right)^2 \\ &= \sum_{j=1}^p \left[\sum_{i=1}^p \left(\left| \Omega_{0,ij} + \frac{u_{ij}}{\sqrt{T}} \right| + |\Omega_{0,ij}| \right) \sum_{i=1}^p \left(\left| \Omega_{0,ij} + \frac{u_{ij}}{\sqrt{T}} \right| - |\Omega_{0,ij}| \right) \right] \\ &= \sum_{j=1}^p \left[\sum_{i=1}^p \left(\left| \Omega_{0,ij} + \frac{u_{ij}}{\sqrt{T}} \right| + |\Omega_{0,ij}| \right) \sum_{i=1}^p \frac{1}{\sqrt{T}} g_{ij} \right] \\ &= \sum_{j=1}^p \left[\sum_{i=1}^p \left(\left| \Omega_{0,ij} + \frac{u_{ij}}{\sqrt{T}} \right| - |\Omega_{0,ij}| + 2|\Omega_{0,ij}| \right) \sum_{i=1}^p \frac{1}{\sqrt{T}} g_{ij} \right] \\ &= \sum_{j=1}^p \left[\left(\sum_{i=1}^p \frac{1}{\sqrt{T}} g_{ij} + \sum_{i=1}^p 2|\Omega_{0,ij}| \right) \sum_{i=1}^p \frac{1}{\sqrt{T}} g_{ij} \right] \\ &= \frac{1}{T} \sum_{j=1}^p \sum_{i,i'=1}^p g_{ij} g_{i'j} + \frac{2}{\sqrt{T}} \sum_{j=1}^p \sum_{i,i'=1}^p |\Omega_{0,ij}| g_{i'j} \end{aligned} \quad (1.15)$$

We can rewrite the second term of equation (1.15) as follows:

$$\begin{aligned}
\sum_{j=1}^p \sum_{i,i'=1}^p g_{ij} |\Omega_{0,i'j}| &= \sum_{j=1}^p \sum_{i,i'=1}^p g_{ij} |\Omega_{0,ji'}| \\
&= \sum_{j=1}^p \sum_{i=1}^p g_{ij} \left(\sum_{i'=1}^p |\Omega_{0,ji'}| \right) \\
&= \sum_{i=1}^p \sum_{j=1}^p g_{ij} d_j,
\end{aligned}$$

where d_j is the true weighted degree of node j defined as $d_j \equiv \sum_{k=1}^p |\Omega_{0,jk}|$.

Combining equations (1.10), (1.13), (1.14) and (1.15), we can write $TV_T(U)$ as

$$\begin{aligned}
TV_T(U) &= \text{tr}(U\Sigma_0 U\Sigma_0) + \text{tr}\left(U\sqrt{T}(\hat{\Sigma} - \Sigma_0)\right) \\
&\quad + \lambda_T \sum_{j=1}^p \sum_{i,i'=1}^p g_{ij} g_{i'j} + 2\sqrt{T}\lambda_T \sum_{i=1}^p \sum_{j=1}^p g_{ij} d_j + o(1)
\end{aligned}$$

In the limit as $T \rightarrow \infty$, we then have:

$$TV_T(U) = \text{tr}(U\Sigma_0 U\Sigma_0) + \text{tr}\left(U\sqrt{T}(\hat{\Sigma} - \Sigma_0)\right) + 2\lambda_0 \sum_{i=1}^p \sum_{j=1}^p g_{ij} d_j$$

Similarly, in the limit as $T \rightarrow \infty$, we have:

$$TV_T^l(U) = \text{tr}(U\Sigma_0 U\Sigma_0) + \text{tr}\left(U\sqrt{T}(\hat{\Sigma} - \Sigma_0)\right) + 2\lambda_0 \sum_{i=1}^p \sum_{j=1}^p g_{ij} d_j$$

Therefore, we have the first result of the theorem.

Under Assumption 3.1 the second result of the theorem follows by the continuous mapping theorem and Lemma 1.1. ■

A.2. Proof of Proposition 3.1

PROOF. Since Ω is symmetric, we have

$$2\|D_p \circ \Omega\|_{1,1} = 2 \sum_{i=1}^p \sum_{j=1}^p d_j |\Omega_{ij}| \tag{1.16}$$

$$\begin{aligned}
&= 2 \sum_{i=2}^p \sum_{j<i}^p d_j |\Omega_{ij}| + 2 \sum_{j=1}^{p-1} \sum_{i>j}^p d_i |\Omega_{ji}| + 2 \sum_{i=1}^p d_i |\Omega_{ii}| \\
&= 2 \sum_{i=2}^p \sum_{j<i}^p d_j |\Omega_{ij}| + 2 \sum_{j=1}^{p-1} \sum_{i>j}^p d_i |\Omega_{ij}| + 2 \sum_{i=1}^p d_i |\Omega_{ii}| \\
&= 2 \sum_{i=2}^p \sum_{j<i}^p d_j |\Omega_{ij}| + 2 \sum_{i=2}^p \sum_{j<i}^p d_i |\Omega_{ij}| + 2 \sum_{i=1}^p d_i |\Omega_{ii}| \\
&= 2 \sum_{i=2}^p \sum_{j<i}^p (d_i + d_j) |\Omega_{ij}| + \sum_{i=1}^p (d_i + d_i) |\Omega_{ii}| \\
&= \sum_{i=1}^p \sum_{j=1}^p (d_i + d_j) |\Omega_{ij}| \tag{1.17}
\end{aligned}$$

B. ILLUSTRATING THE ASYMPTOTIC DISTRIBUTION

We consider the following true precision matrix, Ω_0 . It is an AR(1) model with $p = 4$. The corresponding graph representing Ω_0 is depicted in Figure 6.

$$\Omega_0 = \begin{pmatrix} 1 & 0.5 & 0 & 0 \\ 0.5 & 1 & 0.5 & 0 \\ 0 & 0.5 & 1 & 0.5 \\ 0 & 0 & 0.5 & 1 \end{pmatrix}$$

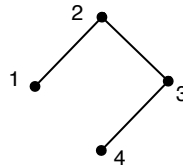


Figure 6: Graph of Ω_0

In Figure 7 here, we illustrate the asymptotic distribution for both GLASSO and SGLASSO, setting $\lambda_0 = 1$ in Theorem 3.1 (see the main text). Each circle in the plot represents a draw from the distribution over $\hat{\Omega}$ as given by Theorem 3.1. Note that the precision matrix is such that $\Omega_{0,13} = \Omega_{0,14} = 0$. For GLASSO, we have $\hat{\Pr}(\hat{\Omega}_{13} = 0) = 0.039$, while for SGLASSO, $\hat{\Pr}(\hat{\Omega}_{13} = 0) = 0.124$. Therefore, SGLASSO does a better job at estimating $\Omega_{0,13} = 0$, where a non-link involves a node of relatively higher degree.

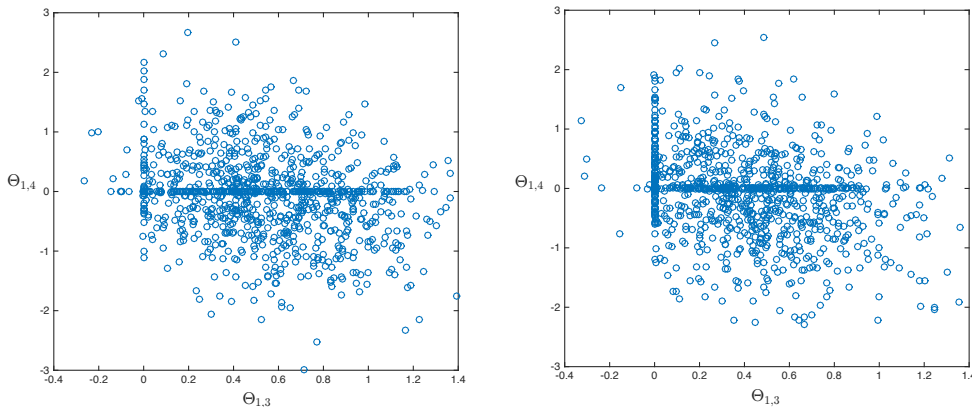


Figure 7: Asymptotic distributions, with $\lambda_0 = 1$. Left-hand side is GLASSO, right-hand side is SGLASSO. For GLASSO, $\hat{\Pr}(\hat{\Omega}_{13} = 0) = 0.039$, $\hat{\Pr}(\hat{\Omega}_{14} = 0) = 0.19$. For SGLASSO, $\hat{\Pr}(\hat{\Omega}_{13} = 0) = 0.124$, $\hat{\Pr}(\hat{\Omega}_{14} = 0) = 0.173$. Standard deviations of both estimators are comparable.

In Figure 8, we show the asymptotic distribution of $\hat{\Omega}$ without any penalty or regularization, which corresponds to the Maximum-Likelihood estimator of the inverse covariance matrix. Comparing the two figures, we see that both $L_{1,1}$ and $L_{1,2}$ norms are able to estimate entries of Ω_0 to be zero exactly, while MLE without regularization fails to recover any sparsity structure.

C. SIMULATION RESULTS

In addition to the 3 graphical models considered in the main text, we explore 8 other models here. The first 10 different graphical models are as depicted in Figures 9 and 10. The last model is the graphical model calibrated to the empirical application. The models in Figure 9 has 5 nodes ($p = 5$), and the models in Figure 10 has 10 nodes ($p = 10$). From a given graphical

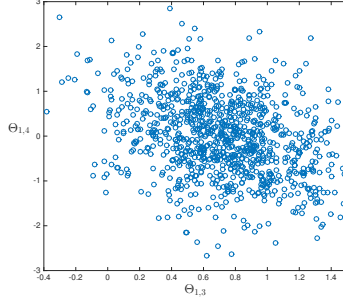


Figure 8: Asymptotic distribution of the Maximum Likelihood Estimator (MLE). This corresponds to the case where $\lambda_0 = 0$.

model, we generate the true precision matrix Ω_0 such that $\Omega_{0,ij} = 0$ if and only if there is a link between nodes i and j , otherwise we set $\Omega_{0,ij} = 0.2$. We set $\Omega_{0,ii} = 1$.

For each model, we draw 1,000 independent datasets from $N(0, \Omega_0^{-1})$. That is, each dataset comprises of $(\mathbf{X}_t)_{t=1}^T$, where $\mathbf{X}_t \in \mathbb{R}^p$ is randomly drawn from $N(0, \Omega_0^{-1})$. Here, our sample size is $T = 20$ when $p = 5$ and $T = 50$ when $p = 10$. For each of the 100 dataset, we use our estimator, as well as the GLASSO, to estimate the underlying inverse covariance matrix.

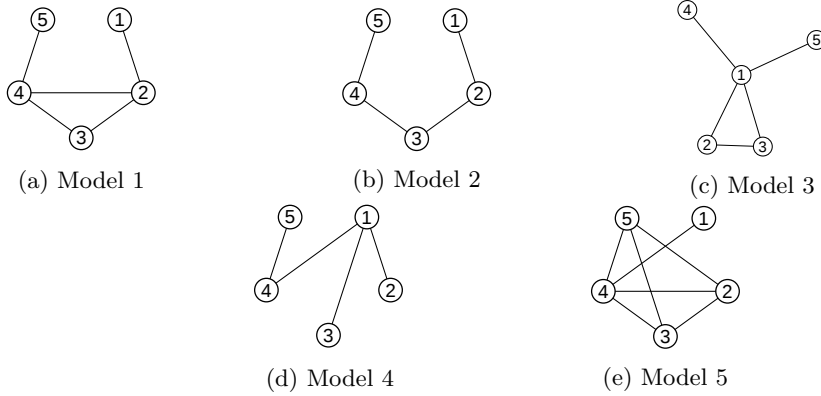


Figure 9: $p = 5$

Both estimators involve choosing the λ_T tuning parameters. We use a 2-folds cross-validation procedure to tune λ_T . Specifically, we use the Kullback-Leibler (KL) loss averaged over the two-folds to evaluate predictive accuracies. Equation (3.18) gives the KL loss between the estimated $\hat{\Omega}$ from the training set versus the estimated Ω from the validation set.

$$KL(\lambda_T) = \log \det(\Omega) - \log \det \hat{\Omega} + \text{tr}(\hat{\Omega} \Omega^{-1}) - p \quad (3.18)$$

We report the simulation result in Table 4 for $T = 20$ and Table 5 for $T = 50$. In the table, the (a) columns corresponds to SGLASSO whereas the (b) columns refer to GLASSO. In Columns 1(a) and 1(b), we report the optimal λ_T as determined by cross-validations, averaged across the 1,000 replications. In Columns 2(a) and 2(b), we report the Kullback-Leibler loss averaged across 1,000 replications. The KL loss between $\hat{\Omega}$ and Ω_0 is given by $KL(\hat{\Omega}, \Omega_0) =$

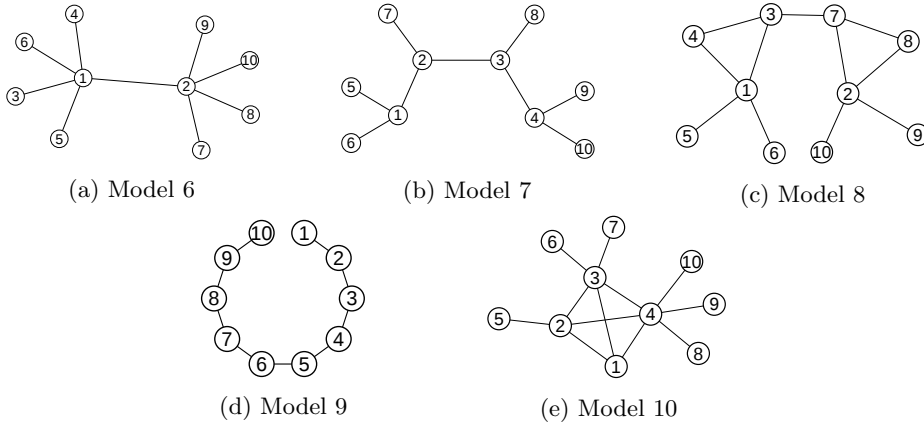


Figure 10: $p = 10$

$\log \det(\Omega_0) - \log \det \hat{\Omega} + \text{tr}(\hat{\Omega}\Omega_0^{-1}) - p$. In Columns 3(a) and 3(b), we report the average Frobenius loss between $\hat{\Omega}$ and Ω_0 .

In the last two columns of Tables 4 and 5, we report the accuracy of graph recovery using SGLASSO and GLASSO. The Kullback-Leibler loss and the Frobenius norms may not fully capture how accurately the zeros are recovered. We introduce an additional metric: F_1 score is $F_1 = \frac{2 \text{precision} \cdot \text{recall}}{\text{precision} + \text{recall}}$, where *precision* is the ratio of true positives (TP) to all predicted positives (TP + FP), *recall* is the ratio of true positives to all actual positives (TP + FN). The notations are further explained in the confusion matrix in Table 3. Alternatively, the F_1 score can be written as $F_1 = \frac{2TP}{2TP + FP + FN}$.

| | Predicted value is 1 | Predicted value is 0 |
|-------------------|----------------------|----------------------|
| Actual value is 1 | True positive (TP) | False negative (FN) |
| Actual value is 0 | False positive (FP) | True negative (TN) |

Table 3: Confusion matrix

Hence, the F_1 score measures the quality of a binary classifier by equally balancing both the precision and the recall of a classifier. The larger the F_1 score is, the better the classifier is. The F_1 score is commonly used in machine learning to evaluate binary classifiers. For instance, the Yelp competition uses the F_1 score as a metric to rank competing models.⁸ The F_1 score is favored over the metric $Accuracy = \frac{TP + TN}{TP + TN + FP + FN}$ especially in our current setting where the graphical models are sparse. This is because a model that naively predicts all negatives will obtain a high *Accuracy* score just because there are many actual negatives, and the TN term dominates the *Accuracy* score.

The conclusion from Tables 4 and 5 is that SGLASSO achieves significantly lower KL and Frobenius losses across all models. Moreover in in terms of graph accuracy, SGLASSO also outperforms GLASSO, as indicated by the F_1 scores. We also observe that as we increase $T = 20$ to $T = 50$, the optimal tuning parameter λ decreases, the KL and Frobenius losses also decrease, while the F_1 score increases. This makes sense because the likelihood becomes more informative as the sample size increases, and therefore the need for regularization decreases.

⁸<https://www.kaggle.com/c/yelp-restaurant-photo-classification>

C.1. Minimum Kullback-Leibler losses

To abstract away from the effects of cross-validations, we consider the lowest Kullback-Leibler losses that can be achieved by our estimator versus the GLASSO. Specifically, we vary λ_T and at each λ_T , we compute the KL and Frobenius losses between the true Ω_0 and $\hat{\Omega}$. We see from Table 7 that the superior performance of SGLASSO over GLASSO exists after taking away the randomness due to cross-validations. The lowest possible KL losses achievable by our estimator appears to be smaller, than the corresponding KL losses for the GLASSO.

C.1.1. Recovering high-degree sparsities Theorem 3.1 says that the SGLASSO prioritizes recovering the sparsity between nodes that have higher degrees. We now show some numerical evidence that lends support to this. For each model, we examined the pair of nodes (i, j) such that $d_i + d_j$ is largest and $\Omega_{0,ij} = 0$, where $d_i = \sum_{k=1}^p |\Omega_{0,ik}|$ is the true weighted degree of node i . For instance, for model 1, the $\text{argmax}_{i,j}(d_i + d_j)$ such that $\Omega_{0,ij} = 0$ would correspond to the pairs of nodes (1, 4) and (2, 5). For simplicity, if there are multiple pairs of nodes that maximize $d_i + d_j$, we will pick the pair of nodes that comes first when the adjacency matrix is vectorized.

In each of the model (set $T = 20$), we calculate the fraction of times that GLASSO and SGLASSO correctly recover $\Omega_{0,ij} = 0$ for the largest $d_i + d_j$. We plot this result in Figure 11, which shows that at any given λ , the probability of correctly recovering $\Omega_{0,ij} = 0$ for high-degree nodes is greater when SGLASSO is used, compared to GLASSO.

| Model | Optimal λ_T | | KL | | Frobenius | | F_1 score | |
|-------|---------------------|------------------|------------------|------------------|------------------|------------------|------------------|------------------|
| | (a) | (b) | (a) | (b) | (a) | (b) | (a) | (b) |
| | SGLASSO | GLASSO | SGLASSO | GLASSO | SGLASSO | GLASSO | SGLASSO | GLASSO |
| (1) | 0.181 (0.118) | 0.342 (0.133) | 0.430 (0.207) | 0.483 (0.215) | 0.896 (0.223) | 0.948 (0.214) | 0.439 (0.248) | 0.367 (0.259) |
| (2) | 0.180 (0.118) | 0.341 (0.136) | 0.419 (0.205) | 0.469 (0.215) | 0.858 (0.232) | 0.906 (0.226) | 0.400 (0.254) | 0.349 (0.276) |
| (3) | 0.183 (0.119) | 0.345 (0.138) | 0.438 (0.210) | 0.492 (0.206) | 0.904 (0.216) | 0.956 (0.204) | 0.415 (0.240) | 0.353 (0.262) |
| (4) | 0.181 (0.119) | 0.341 (0.137) | 0.422 (0.223) | 0.471 (0.208) | 0.859 (0.234) | 0.905 (0.210) | 0.396 (0.253) | 0.325 (0.274) |
| (5) | 0.188 (0.121) | 0.348 (0.138) | 0.453 (0.195) | 0.504 (0.204) | 0.985 (0.189) | 1.032 (0.181) | 0.436 (0.262) | 0.349 (0.270) |
| (6) | 0.203 (0.095) | 0.397 (0.106) | 0.913 (0.270) | 1.050 (0.446) | 1.248 (0.172) | 1.340 (0.312) | 0.332 (0.153) | 0.296 (0.172) |
| (7) | 0.206 (0.094) | 0.398 (0.110) | 0.909 (0.289) | 1.067 (0.579) | 1.264 (0.204) | 1.377 (0.507) | 0.314 (0.141) | 0.274 (0.163) |
| (8) | 0.210 (0.098) | 0.402 (0.110) | 0.939 (0.287) | 1.089 (0.555) | 1.327 (0.192) | 1.431 (0.431) | 0.308 (0.145) | 0.261 (0.160) |
| (9) | 0.208 (0.098) | 0.400 (0.109) | 0.936 (0.297) | 1.089 (0.624) | 1.291 (0.202) | 1.397 (0.470) | 0.317 (0.149) | 0.260 (0.161) |
| (10) | 0.207 (0.094) | 0.399 (0.109) | 0.946 (0.278) | 1.096 (0.527) | 1.353 (0.183) | 1.456 (0.414) | 0.336 (0.143) | 0.272 (0.162) |
| (11) | 0.198 (0.097) | 0.389 (0.117) | 1.201 (0.312) | 1.390 (0.723) | 1.569 (0.186) | 1.701 (0.522) | 0.403 (0.143) | 0.341 (0.164) |

Table 4: Averages and standard errors from 1,000 replications, $T = 20$. Columns 1(a) and 1(b) report the optimal λ_T as determined from cross-validation for (a) SGLASSO and (b) GLASSO. Columns 2(a) and 2(b) are the average Kullback-Leibler losses. Columns 3(a) and 3(b) report the average Frobenius losses. The last two columns report the F_1 scores, which is a metric for how accurately the graphical model is estimated.

| Model | Optimal λ_T | | KL | | Frobenius | | F_1 score | |
|-------|---------------------|------------------|------------------|------------------|------------------|------------------|------------------|------------------|
| | (a) SGLASSO | (b) GLASSO | (a) SGLASSO | (b) GLASSO | (a) SGLASSO | (b) GLASSO | (a) SGLASSO | (b) GLASSO |
| (1) | 0.088 (0.054) | 0.179 (0.076) | 0.246 (0.084) | 0.265 (0.091) | 0.710 (0.129) | 0.736 (0.134) | 0.564 (0.225) | 0.541 (0.248) |
| (2) | 0.090 (0.052) | 0.183 (0.075) | 0.232 (0.083) | 0.252 (0.090) | 0.663 (0.127) | 0.692 (0.130) | 0.548 (0.233) | 0.517 (0.248) |
| (3) | 0.090 (0.053) | 0.181 (0.077) | 0.249 (0.083) | 0.269 (0.091) | 0.715 (0.124) | 0.744 (0.131) | 0.565 (0.215) | 0.530 (0.239) |
| (4) | 0.090 (0.053) | 0.183 (0.076) | 0.234 (0.086) | 0.256 (0.095) | 0.666 (0.127) | 0.696 (0.135) | 0.540 (0.222) | 0.504 (0.250) |
| (5) | 0.089 (0.054) | 0.181 (0.079) | 0.268 (0.081) | 0.290 (0.092) | 0.800 (0.125) | 0.831 (0.138) | 0.568 (0.228) | 0.521 (0.252) |
| (6) | 0.106 (0.038) | 0.228 (0.050) | 0.557 (0.118) | 0.615 (0.132) | 1.024 (0.109) | 1.076 (0.116) | 0.485 (0.135) | 0.479 (0.160) |
| (7) | 0.109 (0.040) | 0.230 (0.048) | 0.551 (0.109) | 0.607 (0.119) | 1.030 (0.109) | 1.084 (0.111) | 0.453 (0.145) | 0.437 (0.156) |
| (8) | 0.110 (0.040) | 0.231 (0.050) | 0.583 (0.114) | 0.642 (0.129) | 1.105 (0.112) | 1.160 (0.117) | 0.457 (0.128) | 0.419 (0.147) |
| (9) | 0.109 (0.040) | 0.230 (0.050) | 0.577 (0.106) | 0.635 (0.118) | 1.061 (0.111) | 1.117 (0.114) | 0.460 (0.137) | 0.438 (0.158) |
| (10) | 0.109 (0.040) | 0.230 (0.052) | 0.593 (0.115) | 0.651 (0.128) | 1.137 (0.113) | 1.190 (0.117) | 0.466 (0.136) | 0.437 (0.159) |
| (11) | 0.091 (0.041) | 0.206 (0.053) | 0.747 (0.153) | 0.807 (0.167) | 1.312 (0.128) | 1.370 (0.133) | 0.563 (0.120) | 0.541 (0.137) |

Table 5: Averages and standard errors from 1,000 replications, $T = 50$. Columns 1(a) and 1(b) report the optimal λ_T as determined from cross-validation for (a) SGLASSO and (b) GLASSO. Columns 2(a) and 2(b) are the average Kullback-Leibler losses. Columns 3(a) and 3(b) report the average Frobenius losses. The last two columns report the F_1 scores, which is a metric for how accurately the graphical model is estimated.

| Model | Minimum KL | | Minimum Frobenius | | Percentage Dominance |
|-------|------------------|------------------|----------------------|------------------|-------------------------|
| | (a) | (b) | (a) | (b) | |
| | SGLASSO | GLASSO | SGLASSO | GLASSO | |
| (1) | 0.340 (0.106) | 0.376 (0.120) | 0.779 (0.096) | 0.821 (0.116) | 0.99 |
| (2) | 0.324 (0.107) | 0.361 (0.120) | 0.734 (0.102) | 0.780 (0.121) | 0.99 |
| (3) | 0.341 (0.105) | 0.378 (0.119) | 0.778 (0.095) | 0.821 (0.115) | 0.98 |
| (4) | 0.326 (0.106) | 0.362 (0.120) | 0.734 (0.102) | 0.779 (0.121) | 0.99 |
| (5) | 0.362 (0.104) | 0.399 (0.118) | 0.873 (0.081) | 0.908 (0.099) | 0.98 |
| (6) | 0.789 (0.162) | 0.846 (0.172) | 1.134 (0.092) | 1.177 (0.103) | 0.99 |
| (7) | 0.771 (0.159) | 0.831 (0.168) | 1.136 (0.091) | 1.182 (0.102) | 1.00 |
| (8) | 0.805 (0.158) | 0.865 (0.168) | 1.199 (0.087) | 1.242 (0.097) | 1.00 |
| (9) | 0.800 (0.161) | 0.860 (0.172) | 1.166 (0.091) | 1.211 (0.100) | 1.00 |
| (10) | 0.824 (0.162) | 0.887 (0.176) | 1.234 (0.085) | 1.279 (0.101) | 0.99 |
| (11) | 1.041 (0.191) | 1.102 (0.205) | 1.415 (0.087) | 1.466 (0.101) | 0.95 |

Table 6: $T = 20$. Minimum possible KL and Frobenius losses across all λ_T . The numbers reported are the average KL and Frobenius losses evaluated at the λ_T that result in the lowest possible values. Standard deviations across 1,000 replications are reported in parentheses. In the last column, we report the fraction of times in which SGLASSO performed better in terms of KL loss at the corresponding λ_T .

| Model | Minimum KL | | Minimum Frobenius | | Percentage Dominance |
|-------|------------------|------------------|----------------------|------------------|-------------------------|
| | (a) | (b) | (a) | (b) | |
| | SGLASSO | GLASSO | SGLASSO | GLASSO | |
| (1) | 0.199 (0.063) | 0.211 (0.065) | 0.606 (0.095) | 0.634 (0.098) | 0.92 |
| (2) | 0.185 (0.059) | 0.198 (0.066) | 0.575 (0.088) | 0.596 (0.102) | 0.87 |
| (3) | 0.198 (0.062) | 0.210 (0.064) | 0.606 (0.093) | 0.632 (0.096) | 0.93 |
| (4) | 0.184 (0.058) | 0.197 (0.064) | 0.575 (0.086) | 0.596 (0.100) | 0.85 |
| (5) | 0.218 (0.063) | 0.231 (0.069) | 0.679 (0.086) | 0.697 (0.098) | 0.94 |
| (6) | 0.468 (0.091) | 0.488 (0.100) | 0.916 (0.078) | 0.931 (0.090) | 0.90 |
| (7) | 0.465 (0.091) | 0.491 (0.098) | 0.917 (0.081) | 0.940 (0.089) | 0.99 |
| (8) | 0.497 (0.085) | 0.522 (0.093) | 0.987 (0.073) | 1.005 (0.083) | 0.96 |
| (9) | 0.485 (0.091) | 0.512 (0.097) | 0.940 (0.080) | 0.964 (0.085) | 0.99 |
| (10) | 0.509 (0.087) | 0.533 (0.095) | 1.021 (0.072) | 1.035 (0.082) | 0.96 |
| (11) | 0.652 (0.104) | 0.675 (0.114) | 1.203 (0.067) | 1.204 (0.082) | 0.86 |

Table 7: $T = 50$. Minimum possible KL and Frobenius losses across all λ_T . The numbers reported are the average KL and Frobenius losses evaluated at the λ_T that result in the lowest possible values. Standard deviations across 1,000 replications are reported in parentheses. In the last column, we report the fraction of times in which SGLASSO performed better in terms of KL loss at the corresponding λ_T .

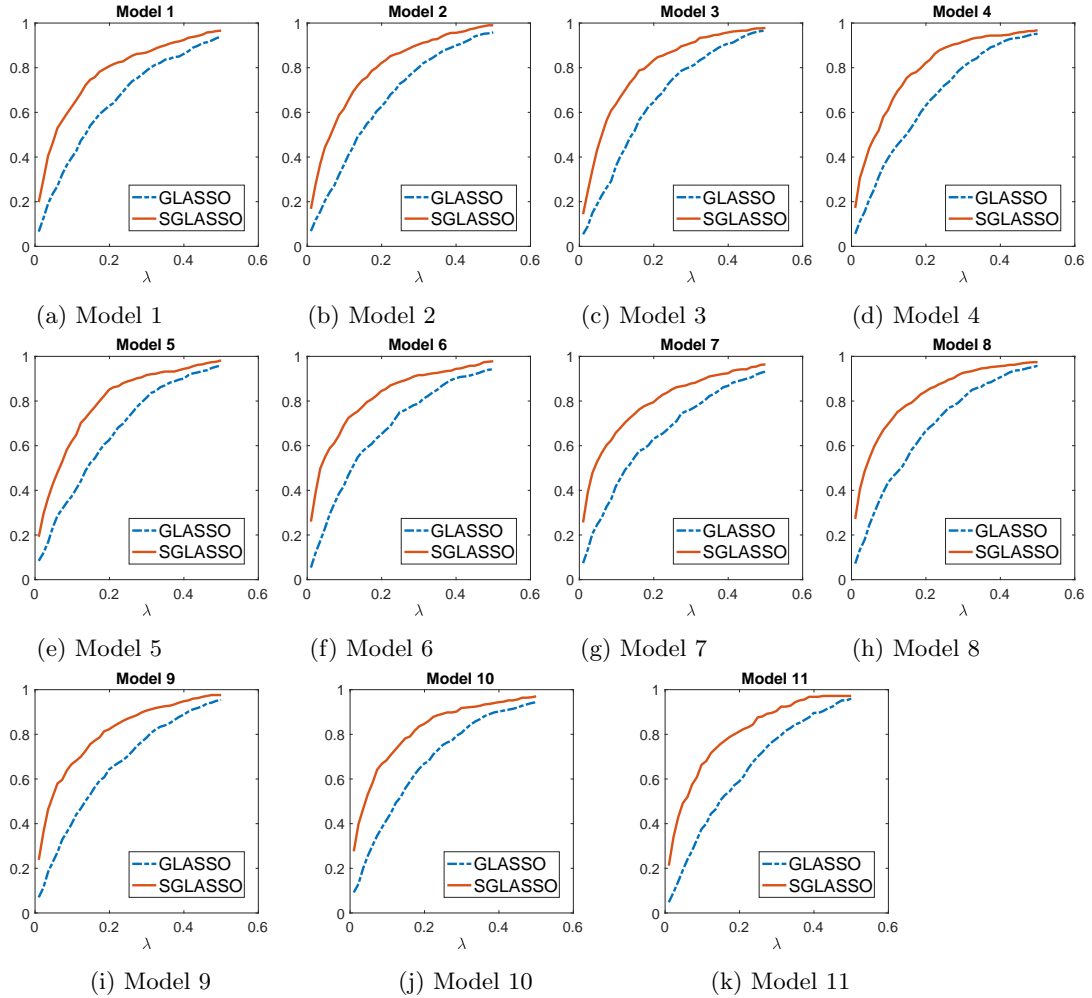


Figure 11: Each figure shows the estimated probability of recovering the non-link (i, j) such that $(d_i + d_j)$ is the largest in each model, as a function of the tuning parameter λ_T . More precisely, for a given λ_T , we calculate the number of times (out of the 1,000 replications) that SGLASSO and GLASSO successfully estimate the entry Ω_{ij} as zero, where (i, j) is such that $\Omega_{0i,j} = 0$ and that $d_i + d_j$ has the highest value among all non-links.

REFERENCES

- Acemoglu, D., V. M. Carvalho, A. Ozdaglar, and A. Tahbaz-Salehi (2012). The network origins of aggregate fluctuations. *Econometrica* 80(5), 1977–2016.
- Baltagi, B. (2008). *Econometric analysis of panel data*. John Wiley & Sons.
- Banerjee, O., L. El Ghaoui, and A. d’Aspremont (2008). Model selection through sparse maximum likelihood estimation for multivariate gaussian or binary data. *The Journal of Machine Learning Research* 9, 485–516.
- Beck, A. and M. Teboulle (2009). A fast iterative shrinkage-thresholding algorithm for linear inverse problems. *SIAM journal on imaging sciences* 2(1), 183–202.
- Belloni, A., V. Chernozhukov, and C. Hansen (2014). Inference on treatment effects after selection among high-dimensional controls. *The Review of Economic Studies* 81(2), 608–650.
- Cai, T., W. Liu, and X. Luo (2011). A constrained ℓ_1 minimization approach to sparse precision matrix estimation. *Journal of the American Statistical Association* 106(494), 594–607.
- Cai, T. T., W. Liu, H. H. Zhou, et al. (2016). Estimating sparse precision matrix: Optimal rates of convergence and adaptive estimation. *The Annals of Statistics* 44(2), 455–488.
- Elliott, M., B. Golub, and M. O. Jackson (2014). Financial networks and contagion. *The American economic review* 104(10), 3115–3153.
- Fan, J. and R. Li (2001). Variable selection via nonconcave penalized likelihood and its oracle properties. *Journal of the American statistical Association* 96(456), 1348–1360.
- Fan, J., Y. Liao, and H. Liu (2015). An overview on the estimation of large covariance and precision matrices. *arXiv preprint arXiv:1504.02995*.
- Fan, J., Y. Liao, and H. Liu (2016). An overview of the estimation of large covariance and precision matrices. *The Econometrics Journal* 19(1), C1–C32.
- Fan, Y. and J. Lv (2016). Innovated scalable efficient estimation in ultra-large gaussian graphical models. *arXiv preprint arXiv:1605.03313*.
- Friedman, J., T. Hastie, and R. Tibshirani (2008). Sparse inverse covariance estimation with the graphical lasso. *Biostatistics* 9(3), 432–441.
- Friedman, J., T. Hastie, and R. Tibshirani (2010). A note on the group lasso and a sparse group lasso. *arXiv preprint arXiv:1001.0736*.
- Geyer, C. J. (1994). On the asymptotics of constrained m-estimation. *The Annals of Statistics*, 1993–2010.
- Giudici, P. and A. Spelta (2016). Graphical network models for international financial flows. *Journal of Business & Economic Statistics* 34(1), 128–138.
- Grant, M., S. Boyd, and Y. Ye (2008). Cvx: Matlab software for disciplined convex programming.
- Grant, M. C. and S. P. Boyd (2008). Graph implementations for nonsmooth convex programs. In *Recent advances in learning and control*, pp. 95–110. Springer.
- Greene, W. H. (2012). *Econometric analysis* (7th ed.). Prentice hall.
- Hastie, T., R. Tibshirani, and M. Wainwright (2015). *Statistical learning with sparsity*. CRC press.
- Hjort, N. L. and D. Pollard (2011). Asymptotics for minimisers of convex processes. *arXiv preprint arXiv:1107.3806*.
- Jackson, M. O. (2008). *Social and economic networks*. Princeton University Press.
- Kato, K. (2009). Asymptotics for argmin processes: Convexity arguments. *Journal of Multivariate Analysis* 100(8), 1816–1829.

- Lam, C. and J. Fan (2009). Sparsistency and rates of convergence in large covariance matrix estimation. *Annals of statistics* 37(6B), 4254.
- Meinshausen, N. and P. Bühlmann (2006). High-dimensional graphs and variable selection with the lasso. *The annals of statistics*, 1436–1462.
- Peng, J., P. Wang, N. Zhou, and J. Zhu (2012). Partial correlation estimation by joint sparse regression models. *Journal of the American Statistical Association*.
- Pollard, D. (1991). Asymptotics for least absolute deviation regression estimators. *Econometric Theory* 7(02), 186–199.
- Ravikumar, P., M. J. Wainwright, G. Raskutti, B. Yu, et al. (2011). High-dimensional covariance estimation by minimizing ℓ_1 -penalized log-determinant divergence. *Electronic Journal of Statistics* 5, 935–980.
- Ren, Z., T. Sun, C.-H. Zhang, H. H. Zhou, et al. (2015). Asymptotic normality and optimalities in estimation of large gaussian graphical models. *The Annals of Statistics* 43(3), 991–1026.
- Rothman, A. J., P. J. Bickel, E. Levina, and J. Zhu (2008). Sparse permutation invariant covariance estimation. *Electronic Journal of Statistics* 2, 494–515.
- Van de Geer, S., P. Bühlmann, Y. Ritov, R. Dezeure, et al. (2014). On asymptotically optimal confidence regions and tests for high-dimensional models. *The Annals of Statistics* 42(3), 1166–1202.
- Whittaker, J. (2009). *Graphical Models in Applied Multivariate Statistics*. London: Wiley Publishing.
- Yuan, M. and Y. Lin (2006). Model selection and estimation in regression with grouped variables. *Journal of the Royal Statistical Society: Series B (Statistical Methodology)* 68(1), 49–67.
- Yuan, M. and Y. Lin (2007). Model selection and estimation in the gaussian graphical model. *Biometrika* 94(1), 19–35.